Princeton Plasma Physics Laboratory

PPPL- 4855

PPPL- 4855

Scrape-off Layer Flows with Pressure Gradient Scale Length ~ ρ_p

Robert J. Goldston

March, 2013

PPPL PRINCETON PLASMA PHYSICS LABORATORY

Prepared for the U.S. Department of Energy under Contract DE-AC02-09CH11466.

P1-015

Scrape-off layer flows with pressure gradient scale length ~ ρ_p

Robert J. Goldston*

Princeton Plasma Physics Laboratory

Abstract

A heuristic model for the plasma scrape-off width balances magnetic drifts against parallel loss at c_s /2, resulting in a SOL width ~ ρ_p. T_{sep} is calculated from Spitzer–Härm parallel thermal conduction. This results in a prediction for the power scrape-off width in quantitative agreement both in magnitude and scaling with recent experimental data. To achieve the ~ c_s /2 flow assumed in this model and measured experimentally sets requirements on the ratio of upstream to total SOL particle sources, relative to the square-root of the ratio of target to upstream temperature. The Pfisch-Schlüter model for equilibrium flows has been modified to allow near-sonic flows, appropriate for gradient scale lengths of order ρ_p, resulting in a new quadrupole radial flow pattern. The strong parallel flows and plasma charging implied by this model suggest a mechanism for H-mode transition, consistent with many observations.

PACS: 52.40.Hf, 52.55.Fa, 52.55.Pi

PSI-20 keywords: Divertor, Divertor modeling, Divertor plasma, Edge modeling, Edge plasma

**Corresponding author address:* Princeton Plasma Physics Laboratory, MS-41, Princeton NJ, 08543, USA

**Corresponding author email:* rgoldston@pppl.gov

Presenting Author: Robert J. Goldston

Presenting Author email: rgoldston@pppl.gov

Scrape-off Layer flows with pressure gradient scale length ~ ρ_p

Robert J. Goldston, Princeton Plasma Physics Laboratory

Introduction

A heuristic drift-based (HD) model has been developed [1] for the power scrape-off layer (SOL) width in low-gas-puff H-mode tokamaks. It balances ~1/2 sound speed parallel flow against grad B and curv B drifts to find: $\lambda \sim 2q\rho_L \sim 2(a/R)\rho_p$. The edge temperature required to evaluate ρ_p is determined by assuming that the dominant energy loss from the SOL is by Spitzer parallel electron thermal conduction, consistent with much reported experimental data. This gives a closed-form solution for λ:

$$\lambda = 5671 \cdot P_{SOL}^{1/8} \frac{\left(1+\kappa^2\right)^{5/8} a^{17/8} B^{1/4}}{I_p^{9/8} R} \left(\frac{2\bar{A}}{\bar{Z}^2\left(1+\bar{Z}\right)}\right)^{7/16} \left(\frac{Z_{eff}+4}{5}\right)^{1/8} \frac{R\left\langle B_p \right\rangle}{\left(RB_p\right)_{omp}} \quad all\ units\ S.I. \qquad \text{(eq. 1)}$$

When compared with the exponential component of outer divertor heat flux, mapped to the outer midplane, the agreement in magnitude and scaling is remarkable (Figures 1 and 2).

The methodology of Ref. 1 is heuristic and the assumptions can be questioned. Nonetheless, since experimental edge electron temperatures are reasonably well predicted by Spitzer conductivity, and come in only to the 1/2 power, it appears incontrovertible that the power scrape-off width in these low-gas-puff H-mode tokamaks is approximately equal to the poloidal gyro-radius, ρ_p. Alternative mechanisms could be proposed for this. For example if "bursty" transport in the H-mode were to move heat across the separatrix with a radial correlation length of ρ_p and then heat were drained from this region by Spitzer thermal conduction over a longer timescale than the burst time, just before the next "burst" could carry the heat further outwards, it seems that one could find the same result – assuming that the self-consistent $T_{SOL}^{1/2}$ sets ρ_p, thereby closing the loop. Even with a non-neoclassical derivation, such a narrow scrape-off width challenges the underlying assumptions of neoclassical theory in the scrape-off layer. Here we examine the implication due to $\lambda \sim \rho_p$ that there must be near-sonic parallel flows in the SOL.

Sound Speed Parallel Flows

We look at two aspects of parallel flows, those into the divertor and Pfirsch-Schlüter flows. The flow into the divertor can be estimated using a 3-point model including 1) the upstream region above the x point, 2) the location of the x point, and 3) the divertor plate. Defining f_u as the fraction of the total source of particles in the SOL upstream of the x-point (including the divergence of radial flows emerging from the plasma) divided by the total particle source all along the field line, and defining f_T as the ratio of the temperature at the divertor target, T_{target}, to that above the x-point, T_u, we find:

$$\boldsymbol{M}_x = \left(\frac{f_T}{f_u^2}\right)^{1/2} - \left(\frac{f_T}{f_u^2} - 1\right)^{1/2} \quad \text{(eq. 2)}$$

which is illustrated in Figure 3. Thus to obtain the high parallel flow ($M_x \sim 1/2$) assumed in the heuristic model and measured in experiments requires $f_u \sim (f_T/1.5)^{1/2}$. For example, for a high-recycling solution with 75 eV upstream temperature and 3 eV target temperature, the ionization below the x-point can exceed the particle flow past the x-point by a factor of ~5. Alternatively there are low-recycling solutions with high f_T and high f_u that allow high M_x. This simple, purely parallel, flux-tube model should however be challenged with experimental data, since ignoring cross-field transport of particles and momentum is questionable, particularly at the peak of the heat flux. It would be appropriate as well, insofar as possible, to determine whether the experimental data for λ_q under study is consistent with $M_x \sim 1/2$ from this analysis, and – further – whether the data are close enough to the conduction-limited regime, which corresponds to $f_T < 0.8$ for 5% accuracy in the evaluation of $T^{1/2}$ based purely on conduction.

Next we estimate the magnitude of the Pfirsch-Schlüter flows. The balance between the divergence of the particle flows associated with the magnetic drifts and that of the parallel Pfirsch-Schlüter flows, as illustrated in Figure 4, scales as

$$\frac{mv_{th,i}^2}{eBR\lambda} = \frac{\rho_L v_{th,i}}{R\lambda} \sim \frac{u_{\|}}{qR} \Rightarrow \frac{u_{\|}}{v_{th,i}} \sim \frac{q\rho_L}{\lambda} \sim \frac{1}{2} \qquad \text{(eq. 3)}$$

Until the last approximation, where the heuristic-drift-based estimate for λ is introduced (assuming that the power scrape off width is comparable to the pressure scrape off width), this is the same result as from standard Pfirsch-Schlüter fluid theory [2]. The final step should not come as a surprise, since the underlying balance of the divergence of drifts against those of flows is the same as gave rise to the heuristic SOL model with $u_{\|} \sim c_s$. However it does come as a challenge to standard neoclassical theory, which assumes that $\lambda >> q\rho_L$ and far subsonic Pfirsch-Schlüter flows.

Collisionless Gyroviscosity

Since these flows are large, one can expect significant gyroviscous effects even in the absence of dissipation. Classical gyroviscosity has been derived in coordinate independent form [3]. If the approximations appropriate for $\lambda_r \sim \rho_p$: $\nabla_r \sim 1/\rho_p$, $\nabla_p \sim 1/a \sim 1/R$ (no expansion in a/R), $\nabla_{\|} \sim 1/qR$, $u_{\|} \sim c_s$, $u_p \sim c_s/q$, are applied to the result in [3], one finds that the "gyroviscous cancellation" approximation is appropriate. The divergence of the collisionless component of the gyroviscous tensor *cancels* the convective momentum transport due to the magnetization flow. All that remains, then, is a modification to the convective derivative:

$$mn\left(\vec{u} \cdot \vec{\nabla}\right)\vec{u} \rightarrow mn\left(\vec{u}_{gc} \cdot \vec{\nabla}\right)\vec{u} \qquad \text{(eq. 4)}$$

This result that the "gyroviscous cancellation" is valid, even in the relevant regime of extreme radial gradients and sonic flows, may be useful in numerically investigating this regime, which remains difficult using 2-D scrape-off layer codes that include drifts. These codes [2] typically include more complex non-dissipative gyroviscous terms.

Collisionless Pfirsch-Schlüter Flows

The first step in solving for Pfirsch-Schlüter flows is to consider the flow pattern in the absence of dissipation. Dissipation of flows and any temperature gradients (ignored here) drive non-ambipolar transport, which in turn drives the divergence-free parallel flow that assures ambipolarity. These latter steps are not addressed here, but much can be learned from the equations governing the dissipationless flow pattern.

Poloidal force balance gives

$$u_r \approx -\frac{\nabla_p p_i}{en_i B_t} + \frac{m_i u_\parallel^2}{eRB_t}\left(\hat{e}_p \cdot \hat{R}\right) + \frac{E_p}{B_t} = -\frac{\nabla_p p}{en_i B_t} + \frac{m_i u_\parallel^2}{eRB_t}\left(\hat{e}_p \cdot \hat{R}\right) \qquad \text{(eq. 5)}$$

where the second term on the R.H.S. is a consequence of centrifugal force, and the second equality takes into account parallel electron force balance.

Parallel force balance, taking into account gyro-viscosity, using the gyro-viscous cancellation, and including the appropriate geometrical terms, permits elimination of the pressure, giving a relationship amongst the flows:

$$u_r = \frac{m_i}{en_i B}\left[\begin{array}{l} \nabla_p n_i u_\parallel^2 + \dfrac{B}{B_p}\nabla_r n_i u_{r,gc} u_\parallel + \dfrac{B}{B_p}\nabla_p n_i u_{T,gc} u_\parallel \\ + \dfrac{B}{B_p} n_i u_\parallel \left(u_\parallel B_p \nabla_p \dfrac{1}{B} - \dfrac{u_{T,gc}}{B_p}\nabla_p B_p \right) \end{array}\right] \qquad \text{(eq. 6)}$$

The new effect here is in the first term on the R.H.S. It can be simply understood: since isothermal plasma conditions are assumed, the presence of ram pressure requires a density depression. The gradient in the density then gives rise to a parallel (and therefore poloidal) electric field through electron parallel force balance, which causes the radial flow on the L.H.S. (Interestingly, the purely centrifugal effect cancels out of the fluid flows.) The second two terms represent gyroviscosity, while the term in the second line is a consequence of requiring divergenceless flows in this geometry. If we ignore, for the moment, the gyroviscous circulation of momentum, which can be anticipated to spread the flows, but not fundamentally change them, the new implied *quadrupolar* parallel flow pattern which results from closing the new quadrupolar radial flows due to the first term on the R.H.S. with parallel flows is shown in Figure 5.

Discussion

Considering the sum of the flows shown in Figures 4 and 5, it seems plausible that fast Pfirsch-Schlüter flows coupled gyroviscously across the separatrix, and plasma charging due to ion loss to the divertor, the latter analogous to the effect pointed out by Chang *et al.* [4], could drive the sheared flows that quench turbulence and cause the H-mode transition. The total radial particle flow on the outside in major radius is greater than that on the inside. With ion grad *B* drift downwards, a lower single null divertor intercepts a greater ion flow than with ion grad *B* drift upwards (in which all of the arrows reverse). An outer divertor, as on JT-60, stagnates the outer midplane Pfirsch-Schlüter SOL flow that couples viscously to the edge, which could make the H-mode more difficult to attain. Furthermore, the plugging of flow at higher f_T/f_u^2 shown in Figure 3 may be tied to the density dependence of the H-mode threshold power. Recent results on NSTX showing a lowered H-mode power threshold with lithium evaporation may support this, as does the general observation that the H-mode threshold power increases with “gassed up” walls. A potential implication for ITER is that transition to the H-mode may require operation in a high flow, relatively low recycling regime. The large, closed divertor on ITER may make access to this regime more difficult, although the ITER divertor geometry could also provide the benefit of broadening both the upstream λ_q and subsequent spreading of heat flux along the divertor field lines.

Interesting as these preliminary conclusions are, more complete numerical modeling is needed to allow quantitative study of the rapid divertor and Pfirsch-Schlüter flows that arise in the presence radial gradients of order ρ_p, and of their implications.

Acknowledgments

The author wishes to thank Vladimir Rozhansky and Peter Stangeby for very helpful discussions. This research supported by the U.S. Department of Energy under contract DE-AC02-09CH11466.

References

[1] R.J. Goldston, Nucl. Fusion 52 (2012) 013009

[2] V.A. Rozhansky et al., Nuclear Fusion **41** (2001) 387

[3] J.J. Ramos, Phys. Plasmas 12 (2005) 112301

[4] C.S. Chang *et al.,* Physics of Plasmas **9** (2002) 3884

[5] T. Eich et al., “Empirical Scaling of Heat Flux Widths in Tokamaks”, 20’th International Conference on Plasma Surface Interactions, 2012, Aachen, Germany

[6] T. Eich et al., Phy. Rev. Lett. 107 (2011) 215001

Figure Captions

Figure 1. Exponential component of low-field side heat flux mapped to outer midplane, λ_q, from ASDEX, C-MOD, DIII-D, JET, MAST and NSTX [5].

Figure 2. Model prediction, top line, and regression results, bottom line [6]. These represent the scalings predicted by the model and the regression fits to the data for λ_q using the same parameters, with their statistical uncertainties.

Figure 3. Mach number at the *x*-point from three-point model for scrape-off-layer flow. f_u is the fraction of particle source from upstream of the *x*-point, and f_T is the ratio of the target plasma temperature to the upstream plasma temperature.

Figure 4. Ion guiding-center magnetic drifts, flows into the divertor, and Pfirsch-Schlüter flows. Ion grad *B* drift down.

Figure 5. Fluid radial and parallel flows driven by near-sonic Pfirsch-Schlüter flows. Ion grad *B* drift down.

Figures

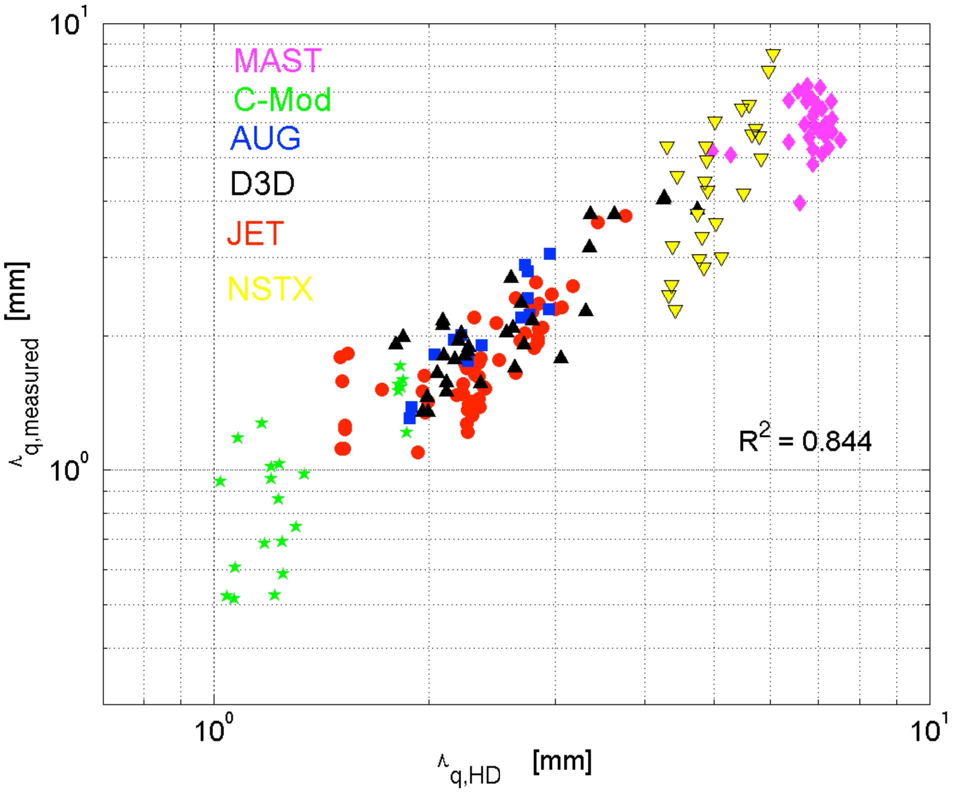

Figure 1.

TABLE III. Summary of regression and model prediction.

	C_0	C_B	C_q	C_P	C_R
λ_m^*	0.92	−0.875	1.125	0.125	0
λ_q	0.73 ± 0.38	−0.78 ± 0.25	1.20 ± 0.27	0.10 ± 0.11	0.02 ± 0.20

Figure 2.

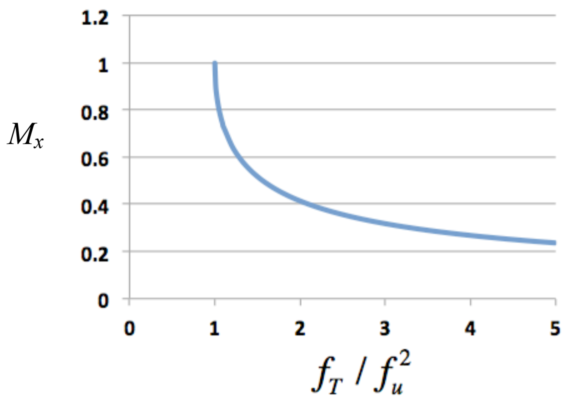

Figure 3.

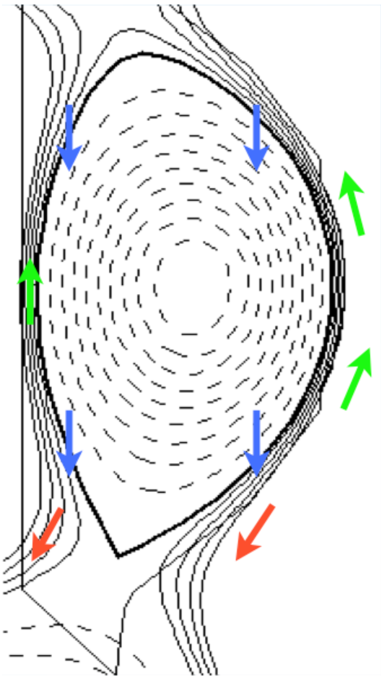

Figure 4.

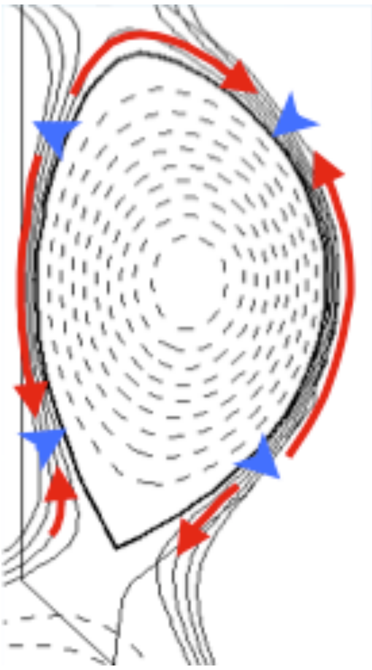

Figure 5.

The Princeton Plasma Physics Laboratory is operated
by Princeton University under contract
with the U.S. Department of Energy.

Information Services
Princeton Plasma Physics Laboratory
P.O. Box 451
Princeton, NJ 08543

Phone: 609-243-2245
Fax: 609-243-2751
e-mail: pppl_info@pppl.gov
Internet Address: http://www.pppl.gov